Determination of the Platinum and Ruthenium Surface Areas in Platinum−Ruthenium Electrocatalysts by Underpotential Deposition of Copper. 2. Effect of Surface Composition on Activity

Clare L. Green and Anthony Kucernak*

Department of Chemistry, Imperial College of Science Technology and Medicine, London SW7 2AY, U.K.

Received: April 1, 2002; In Final Form: July 30, 2002

Submonolayer amounts of Ru have been deposited on a polycrystalline Pt bead electrode from a solution containing 6.68×10^{-4} mol dm^{-3} $RuNO(NO_3)_3$ using an impinging jet apparatus. Deposition of Ru on a platinum surface almost completely covered with H_{ads} due to exchange of the adsorbed hydrogen with Ru^{3+} produces a surface coverage of 0.12 ± 0.02. The reduction of Ru occurs via two separate pathways: in one, metallic Ru is deposited on the surface; in the other, the complex is reduced to an intermediate oxidation state and remains soluble. The latter process, which occurs at potentials less than about 0.25 V has not been previously reported and may explain some of the discrepancies seen in the literature. For characterization of the resultant Pt(Ru) surface we compare the approach developed by Motoo and Watanabe (*J. Electroanal. Chem.* **1975**, *60*, 267−273)[1] and Frelink et al. (*Langmuir* **1996**, *12*, 3702)[2] with that utilizing copper upd. The latter approach is applicable for Ru coverage from 0 up to at least 0.80, whereas the former methods are only applicable up to a coverage of ca. 0.30. On addition of Ru to a clean Pt surface a small initial drop in total surface area is seen, but the area then remains quite constant with increasing Ru coverage. In comparison, the charge measured from stripping of a saturated CO layer adsorbed at 0.3 V(RHE) shows an increase with Ru coverage. The most active surface for the oxidation of an adsorbed CO layer as measured by the potential at which half of the CO has been oxidized is found to contain a Ru surface coverage of 0.2. In comparison, for the oxidation of methanol at 25 °C, it is found that there is a broad maximum in catalytic activity for Ru surface coverage in the range 0.25−0.5. The long term poisoning rate of the electrodes is highly dependent upon Ru coverage, showing a minimum over the range 0.4−0.6.

1. Introduction

The interest in fuel cells for both stationary and mobile power generation is increasing as both industry and governments show their heightened commitment to the ultimate goal of zero-emission energy production.[3,4] Platinum alloy catalysts have been utilized in both solid polymer and phosphoric acid fuel cells (SPFCs and PAFCs, respectively), with hydrogen as the fuel in real examples. The direct methanol fuel cell (DMFC) has a key advantage over hydrogen as a fuel, in that as a liquid, storage and refuelling are much easier and the disadvantages of utilizing a re-former are bypassed. One novel application of this is as the energy source for the "dismounted soldier", enabling a rechargeable power device, namely the direct methanol fuel cell (DMFC), to provide for the total energy requirements of all necessary electronic equipment, with the added benefit of virtually instantaneous recharging.[5]

Platinum−ruthenium catalysts are generally accepted as being the most active toward methanol oxidation. The enhancement over pure platinum is due to the lower potential required for the dissociation of water on ruthenium, thereby allowing more facile oxidation of the carbonaceous adsorbate on adjacent platinum sites. Although PtRu alloys are widely used, the state-of-the-art involves the incorporation of further alloying elements, with both PtRuIr[6] and PtRuIrOs[7] showing significant improvements in comparison with PtRu alone.

The state of the catalyst surface is intrinsic to its activity.[8] This can be considered in terms of two aspects. The first is the proportions in which the different basal planes are present in the catalyst. This has been shown to have a significant effect on oxidation activities. Pt(111) has a much greater activity toward methanol oxidation than polycrystalline platinum[9] and the onset of bulk oxidation decreases in the order Pt(100) > Pt(110) > Pt(111).[10] Similar single-crystal work with ruthenium (sub)monolayers deposited on platinum single crystals found a unique optimum methanol reactivity for a Pt(111)Ru catalyst with 0.2 monolayer of ruthenium present.[9]

This leads to the second aspect, the surface composition of the electrode. This is a significant requirement in the production of efficient catalysts for fuel cell (and other) applications, because, as a result of surface segregation (the enrichment of the surface of an alloy by one component, usually that with the lower heat of sublimation), the bulk composition of the catalyst cannot be assumed to be the same as that of the surface. The surface of PtRu alloys has been shown to be enriched in platinum upon heating to temperatures greater than 300 °C in an inert or reducing atmosphere.[11,12]

In fact, there are several examples in the literature in which PtRu catalysts show a maximum in activity for vastly different bulk compositions. These results may be significantly explained by the two effects mentioned above, especially the latter effect. For PtRu catalysts produced using the Raney method[1] or PtRu catalysts produced from a sulfito precursor[13] a 50−50 atom ratio is found to be the optimum surface composition for methanol

* Corresponding author. E-mail: a.kucernak@ic.ac.uk. Phone: +44 20 75945831. Fax: +44 20 75945804.

10.1021/jp020859y CCC: $22.00
Published on Web 10/10/2002

oxidation at 0.5 V, although, as will be discussed below, the method of determining the surface coverage of Ru in these experiments is questionable. In contrast, the co-electrodeposited PtRu catalyst used by Frelink et al.[14] showed a maximum in activity for a 15% Ru content and the alloy PtRu electrodes used by Gasteiger et al.[15] suggest a maximum performance at 10% Ru. Between these values, studies on Ru electrodeposited onto bulk Pt surfaces suggest that the optimum composition is relatively broad, with the highest activity seen with Ru surface composition in the range 15−50%.[16,17] Indeed, Chrzanowski and Wieckowski have looked at the Ru surface coverage that produces the maximum activity for methanol oxidation on the three major Pt crystallographic faces. The highest Ru coverage is found on the Pt(100) surface (0.30 ± 0.05), with the Pt(111) surface requiring an intermediate coverage (0.20 ± 0.05), and the Pt(110) surface requiring the lowest coverage (0.15 ± 0.03).[18] The Pt(111)/$Ru_{\theta=0.2}$ surface shows the highest activity overall. One further complexity of this analysis is that the optimum surface composition is highly temperature dependent, with increasing temperatures favoring higher Ru coverages.[19]

The determination of the optimum surface composition requires a method of determining what the actual composition is. Ex situ techniques such as XPS, AES, LEIS, and EXAFS are commonly employed[8,9,19,20] but have two main constraints. The first is that they tend not to be in situ and thus it is necessary to transfer the catalyst from the aqueous environment to the high vacuum needed for these techniques. One counter example to this is the use of in situ EXAFS to study fuel cell catalysts.[21] The other aspect is that in real fuel cells the catalysts are highly dispersed and in contact with a solid polymer electrolyte that cannot be removed in the same way that an aqueous electrolyte can. As the solid polymer electrode provides an environment devoid of free anions, it is obvious that there are some differences between the environments within which a real fuel cell catalyst operates and that in which a planar model catalyst surface in contact with an aqueous electrolyte operates.

Various model systems have been developed to study the role of surface Ru in the electrooxidation of both methanol and carbon monoxide. Two approaches of particular interest to this study are the electrodeposition of Ru onto Pt substrates and the simultaneous deposition of PtRu. Chrzanowski and Wieckowski[22] proposed spontaneous deposition of Ru from the $RuCl_3$ complex onto single-crystal (111)−Pt substrates to a maximum coverage of around 20%, a technique that has been used extensively and also reversed to provide the spontaneous deposition of Pt onto Ru substrates.[23,24]

Great efforts have been made to characterize the Ru−Pt system with much work having been carried out on both polycrystalline and single-crystal substrates. Various electrochemical techniques have been used to determine the surface composition of electrodeposited Ru, and of electro-codeposited PtRu. Such methods include a correlation of the size and position of the oxide reduction peak and the electrochemical quartz crystal microbalance signal with Ru surface coverage[2,14,25] and the change in the peak potential for the removal of a monolayer of adsorbed carbon monoxide with Ru coverage.[26] In the latter case the Ru coverage was determined using ex situ methods.[12] The electrochemical technique of utilizing the $Ru(OH)_x$ charge to determine Ru coverage was proposed by Watanabe and Motoo.[1] They suggested that oxidation of surface ruthenium atoms in the double-layer region resulted in the consumption of 1 equiv of charge:

$$Ru + H_2O \rightarrow RuOH + e^- + H^+ \qquad (1)$$

and that as each Ru atom would suppress the adsorption of one hydrogen atom, it was possible to determine the Ru coverage, θ_{Ru}, by

$$\theta_{Ru} = \Delta Q_{Ru-OH}/Q_{Pt-H} \qquad (2)$$

where ΔQ_{Ru-OH} is excess charge seen in the double-layer region due to the oxidation of surface Ru atoms, and Q_{Pt-H} is the charge in the hydrogen adsorption region in the absence of any Ru on the surface. The authors used this approach to characterize a range of electrodeposited PtRu electrodes with $0.2 \leq \theta_{Ru} \leq 0.6$, although they did not give any other supporting evidence for justification of their approach.

More recent research by Frelink et al.[2] used the electrochemical quartz crystal microbalance (EQCMB) technique to study the formation of $Ru(OH)_x$ on platinum electrodes with electrodeposited Ru layers. On the basis of mass change during polarization they concluded that the oxidation of Ru on the surface consumed 2 equiv of charge per ruthenium site, and thus the reaction should be written

$$Ru + 2H_2O \rightarrow Ru(OH)_2 + 2e^- + 2H^+ \qquad (3)$$

from which[14]

$$\theta_{Ru} = \Delta Q_{Ru(OH)_2}/(\Delta Q_{Ru(OH)_2} + 2Q_{PtRu-H}) \qquad (4)$$

where Q_{PtRu-H} is the charge in the hydrogen adsorption region on the Pt−Ru electrode. Both of these approaches might be considered simplistic in light of the work of others on the complex structure of the oxide produced on these materials.[27,28]

We are developing a totally alternative approach to surface area determination involving the use of underpotential deposition of copper.[29] It has been previously shown that a monolayer of copper can be deposited on Pt[30−33] or Ru[34] substrates in a 1:1 ratio and as such the charge passed in removing the deposit is indicative of the underlying surface area. In our recent paper we have shown the use of underpotential deposition of copper may be used as a tool for determining the surface area of high surface area platinum−ruthenium alloy catalysts in contact with the solid polymer electrolyte Nafion. In addition to the overall surface area, we found that by manipulating the conditions used, we could determine the surface coverage of each of the alloying elements.

Our goal in developing this technique is to produce a method that can be used to characterize fuel cell type electrodes in which the high surface area catalyst is in direct contact with a solid polymer electrolyte, and so is thus not amenable to the normal techniques of surface science (except maybe the XAFS technique). This research is driven by the realization that the environment in which the catalysts in fuel cells find themselves is quite different from the typical aqueous environments used to study model (planar) electrocatalysts. Namely, there is the absence of free anions, the water activity is quite different from that of aqueous electrolytes, and there is a highly tortuous interface between the catalyst and the electrolyte.

This paper is divided into three sections. In the first we elaborate a new process for creating platinum surfaces decorated with known coverages of Ru. We have used the $Ru(NO)(NO_3)_3$ complex as the source for the Ru, as we find that we are able to produce a much higher coverage of Ru than reported in the literature for $RuCl_3$-based electrochemical deposition, and also to ensure that the deposits are free of any residual contamination by the coordinating ligands.[35] In the second section we validate the Cu upd approach as previously used on high surface area

catalysts[29] and show how it can be used to characterize these model Pt(Ru) planar catalyst surfaces. In the final section we look at the activity of these surfaces toward CO and methanol oxidation and show how the results match those found on other model catalyst systems. We perform all of our experiments utilizing an impinging jet flow system.[36] The advantage of using the impinging jet method over, for instance, the rotating disk method, is that we maintain solution contact and electrochemical control of the electrode *at all times*, even between the Ru-deposition, characterization, and electrocatalytic measurement stages. Thus there is no need to expose the electrode to the atmosphere or lose electrochemical control due to the need to change electrolyte in the electrochemical cell.

2. Experimental Section

2.1. Chemicals. Solutions were prepared from H_2SO_4 (BDH ARISTAR grade), $CuSO_4 \cdot 5H_2O$ (Aldrich Chemical Co., 99.999%), ruthenium(III) nitrosyl nitrate (Aldrich Chemical Co., Ru 1.5 wt %) and methyl alcohol (Aldrich, 99.9+%, HPLC grade) with deionized water (18 MΩ cm conductance, Millipore MilliQ system). Degassing was carried out using oxygen-free nitrogen (BOC Gases, 99.9999%).

2.2. Electrochemical Experiments. *2.2.1. General Information.* Glassware was soaked in acidified permanganate solution and then rinsed with an $H_2O_2-H_2SO_4$ solution prior to being rinsed with water before all experiments.[37] Purity of the solutions and cleanliness of the glassware was confirmed by less than 5% loss of $Pt-H_{ads}$ charge during a 10-min period of potential cycling between 0 V and halfway along the double-layer region (0.55 V) at 0.1 V s^{-1}.

Unless otherwise stated, the background electrolyte was 0.5 mol dm^{-3} sulfuric acid. All solutions were thoroughly degassed throughout the experiment with nitrogen and a positive pressure of nitrogen was always maintained in the working electrode compartment.

A saturated calomel electrode was used as the reference electrode. Communication to the reference electrode was made by means of a "leaky junction" and all potentials reported in this paper are corrected to the RHE scale. The potentiostat used was an Autolab PSTAT 30 (EcoChemie, Utrecht, Netherlands), with an FI20 current integration module.

The counter electrode was a platinum coil immersed in the bulk cell solution. Contamination of the electrode surface by either chloride ions or species produced at the counter electrode was prevented as a result of the flowing electrolyte.

For the ring−disk voltammetry displayed in Figure 3, a Pine AFMSRX motor controller and ring−disk rotator with a MT28 platinum ring−disk electrode, were used (Pine Instruments Co, PA). The disk was 4.57 mm in diameter (0.1642 cm^2), and the ring had an inner diameter of 4.93 mm and an outer diameter of 5.38 mm (0.037 cm^2). Experiments were performed in collection mode. The collection efficiency of the ring was measured as 21%, close to the theoretical value of 22%.

2.2.2. Impinging Jet Apparatus. All of the results presented in this paper, apart from Figure 3, were obtained using an impinging jet system. This system was utilized to allow the rapid injection and switchover of reactants onto a platinum bead electrode. The system is based on that developed by Bergelin et al.[36,38−40] Experimentation is carried out in the bead of electrolyte that hangs from the electrode surface as a result of the flow directed at it from the impinging tube, Figure 1a. This tube also supports the drop and allows an elongated meniscus to be formed between the electrode and electrolyte surfaces. The flow of electrolyte from the impinging tube to the electrode

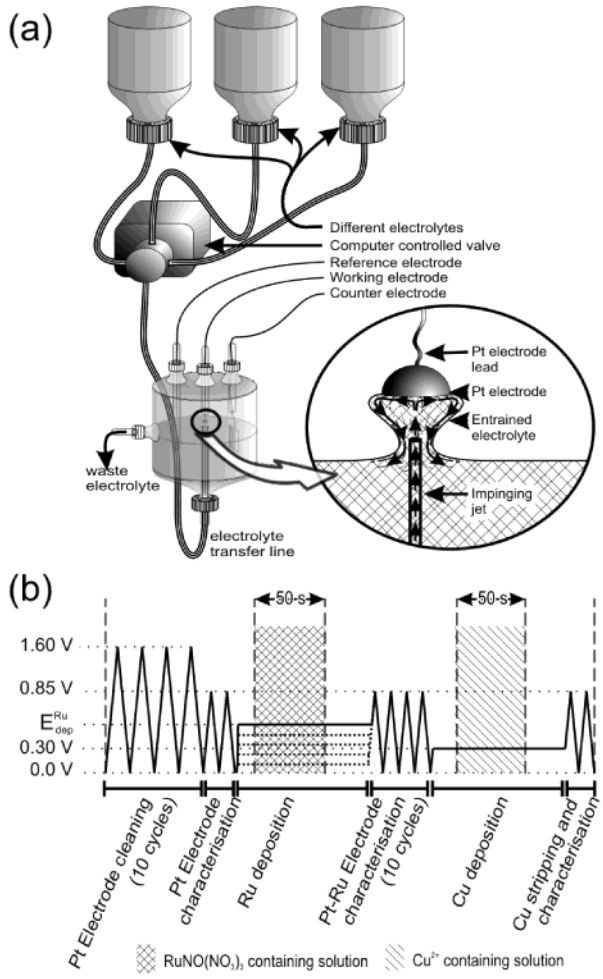

Figure 1. Cartoon of the geometry of the impinging jet apparatus (a). Shown is the impinging jet of the electrolyte and the flow direction of that electrolyte off the working electrode and into the bulk solution. Potential−time profile applied to the platinum electrode during the preparation of Pt(Ru) electrodes (b). The background electrolyte at all times was 0.5 mol dm^{-3} sulfuric acid. During those periods marked $RuNO(NO_3)_3$, the solution also contained 6.68×10^{-4} mol dm^{-3} $RuNO(NO_3)_3$. During those periods marked Cu^{2+}, the solution also contained 1.08×10^{-3} mol dm^{-3} $CuSO_4$.

and into the bulk electrolyte prevents contamination of the flowing electrolyte by the bulk solution. This flow cell configuration allows the dosing of a "probe" species into the flow of clean electrolyte by means of a five-way valve. As such, it permits simple and rapid switching of the electrolyte solution from a background solution to (for example) Ru^{3+}-containing or Cu^{2+}-containing electrolytes while all the time maintaining potential control over the electrode.

The working electrode was a planar polycrystalline platinum disk formed through flame annealing and subsequent polishing of a platinum wire (Advent Metals, 99.995%) and was of diameter 1.59 mm. For all experiments the temperature was 25 °C.

Preparation and characterization of the Pt(Ru) electrodes was performed according to Figure 1b. The platinum electrode was electrochemically cleaned via cycling between 0.0 and 1.60 V in flowing background electrolyte prior to characterization during two cycles between 0.0 and 0.85 V. All scans finished on the positive going sweep at 0.05 V. The potential was then switched to a given value suitable for Ru deposition for 150 s (details given later) and a 50 s dose of the Ru solution was introduced into the electrolyte flow to the electrode. After this

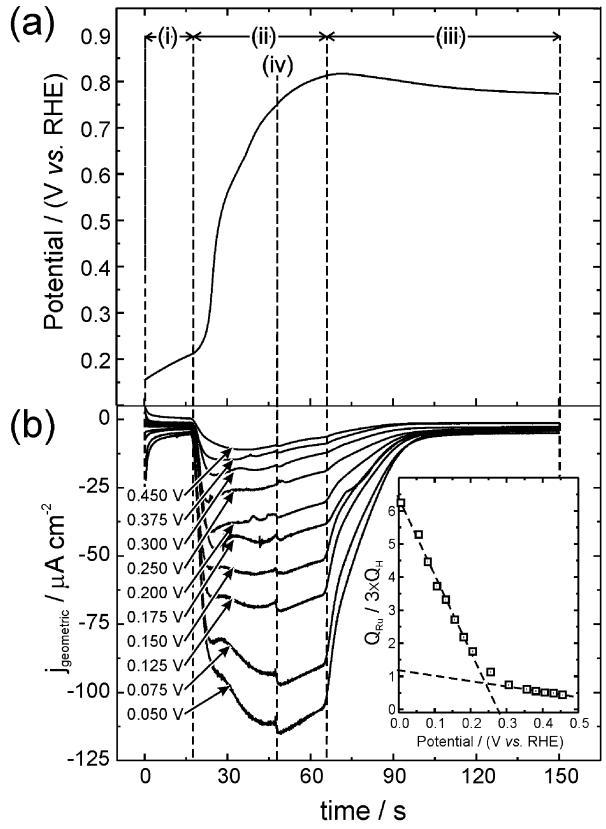

Figure 2. (a) Chronopotentiometry for the spontaneous adsorption of ruthenium from a solution of 6.68×10^{-4} mol dm^{-3} $RuNO(NO_3)_3$ in 0.5 mol dm^{-3} sulfuric acid onto a platinum electrode previously polarized at 0.05 V. (b) Chronoamperometry for the deposition of ruthenium from a solution of 6.68×10^{-4} mol dm^{-3} $RuNO(NO_3)_3$ in 0.5 mol dm^{-3} sulfuric acid onto a platinum electrode as a function of polarization potential. Inset is the ratio of the reduction charge to 3 times the charge corresponding to a monolayer of adsorbed hydrogen. For both (a) and (b) the ruthenium containing solution was injected for 50 s.

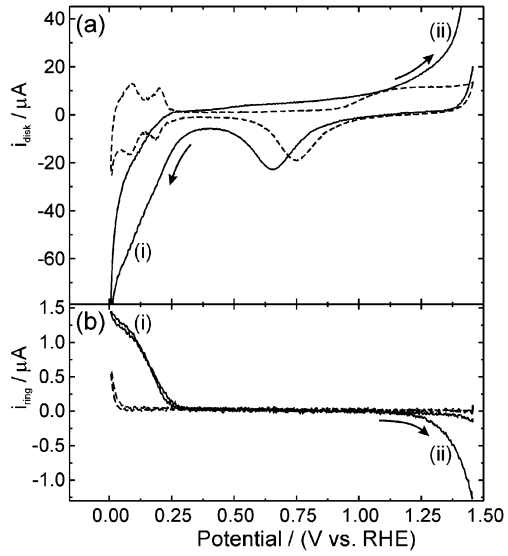

Figure 3. Rotating ring−disk voltammograms in a solution of 0.5 mol dm^{-3} sulfuric acid in the absence (- - -) and presence (—) of 6.17×10^{-4} mol dm^{-3} $RuNO(NO_3)_3$: current on disk (a); current on ring, $E = 0.456$ V (b). $\omega = 60$ Hz. $dV/dt = 0.05$ V s^{-1}.

150 s period the electrode underwent 10 further potential cycles between 0.0 and 0.85 V in flowing background electrolyte with the potential finishing at 0.30 V on the positive scan direction. The upper potential limit during the characterization voltammetric scans was chosen so as to avoid modification of the surface due to platinum oxide growth and to prevent the formation of higher oxidation state oxides of Ru.[28]

The charges corresponding to the processes of interest were found by subtraction of the scan for the electrode with the same composition solely in background electrolyte and integration of the current−voltage curve between the relevant limits. This removes the effect of OH adsorption/oxide growth and double-layer charging from the integrated charges. We make the assumption that the degree of anion adsorption is the same on a Cu_{upd} surface as that on the Pt(Ru) surface.

Removal of ruthenium deposits was accomplished electrochemically by 10 potential cycles between 0.0 and 1.60 V in flowing background electrolyte. This results in oxidation of the ruthenium to a soluble form (probably a derivative of RuO_2) followed by convective removal away from the surface. Complete removal of ruthenium was evident from the reestablishment of an ideal platinum voltammetric response. The reproducibility of cyclic voltammetric curves involving the Ru-covered surfaces was high, showing no difference between experiments. Integrated ruthenium deposition charges for a given electrolysis time displayed a relative scatter of less than 5%. Ruthenium coverage data presented below were obtained as the average of three measurements.

Current densities are specified as either *specific* current densities ($j_{specific}$), i.e., the current divided by the real surface area of the platinum electrode determined by hydrogen adsorption voltammetry, or *geometric* current densities ($j_{geometric}$), i.e., currents divided by the plan surface area of the underlying platinum electrode.

3. Results and Discussion

3.1. Preparation of Pt(Ru) Electrodes. After the electrode was electrochemically cleaned and characterized, different amounts of ruthenium were deposited on the electrode by either allowing the electrode to attain an open circuit potential or explicitly polarizing the electrode at a fixed potential. Deposition of ruthenium occurred following injection of a 50 s pulse of 6.68×10^{-4} mol dm^{-3} $Ru(NO)(NO_3)_3$ solution in 0.5 mol dm^{-3} sulfuric acid into the electrolyte stream. The Ru arrived at the electrode surface within 20 s of injection, as indicated by a rapid increase in the reduction current recorded during chronoamperograms. Complete evacuation of the Ru species from the impinging jet delivery tube was evident from the decay in reduction current in the chronoamperograms. Figure 2 shows both the chronoamperometric and chronopotentiometric transients for the ruthenium deposition. Region (i) corresponds to the period during which background electrolyte flows over the electrode; region (ii) corresponds to the period over which the ruthenium-containing electrolyte flows over the electrode; and region (iii) corresponds to the period over which background electrolyte again flows over the electrode. It takes about 20 s for any change in the composition of the electrolyte to reach the electrode. During this period, there is some mixing at the interface between the two electrolytes, leading to a broadening of the switchover points, at the end of periods i and ii. At point iv, a small jump in the current, clearly evident during the chronoamperometric transients at 50 s, shows the point at which the electrolyte is switched from Ru-containing solution back to the background electrolyte. The transient is due to a slight difference in flow rates between the two solutions used, resulting in a change in the reduction current. The change in flow rate is communicated immediately to the electrode, rather than requiring the 20 s delay seen for changes in electrolyte composition.

3.1.1. Ruthenium Deposition via Ionization of Preadsorbed Hydrogen. Displayed in Figure 2a is the chronopotentiometric transient for a platinum electrode prepolarized at 0.05 V in 0.5 mol dm^{-3} sulfuric acid. Under such conditions the surface is expected to be initially in a reduced state and covered by almost a saturated layer of adsorbed hydrogen. During the period that the ruthenium-containing solution flows over the surface, the potential increases from 0.22 to 0.82 V. Once the ruthenium-containing solution is replaced by background electrolyte, the potential relaxes to 0.78 V. Szabó and Bakos observed qualitatively similar curves on a platinized platinum electrode, although in their case they utilized an $RuCl_3$ solution of higher concentration than that used in our experiments.[41] Interestingly their deposition process required much longer to complete, requiring about 60 min to reach an equilibrium potential of 0.8 V. The difference may very well be due to the much higher roughness factors of their electrodes (ca. 250), and the absence of any convective transport of reactants to the electrode surface.

Spontaneous deposition of an adsorbed ruthenium layer has been noted by Chrzanowski and Wieckowski up to a 20% coverage,[22] but only when aged $RuCl_3$ solutions are used, and not for the case of $RuNO(NO_3)_3$ solutions, indicating that the latter complex is more stable, and less likely to spontaneously adsorb onto the platinum electrode surface. At 0.05 V, we calculate that the adsorbed hydrogen layer is 95% complete from the integrated background corrected voltammetry of the Pt electrode in sulfuric acid electrolyte. The spontaneous deposition of Ru will be driven by the exchange of adsorbed hydrogen atoms with the soluble $RuNO(NO_3)_3$ complex:

$$PtH_{ads} \rightarrow Pt + H^+ + e^- \qquad (5)$$

$$RuNO(NO_3)_3 + 3e^- \rightarrow Ru + NO + 3NO_3^- \qquad (6)$$

although, as will be shown below, the second process does not take place in a single step, and may result in the formation of soluble Ru^{I} or Ru^{II} species that will be lost to the solution, a possibility that has received little consideration in the literature. Thus, the surface coverage of Ru on the Pt electrode after exposure to the Ru-containing solution would be less than the 32% expected if all of the hydrogen charge were used to deposit Ru.

3.1.2. Chronoamperometric Deposition of Ruthenium. Typical chronoamperograms as a function of deposition potential are displayed in Figure 2b. It can be seen that as the deposition potential is decreased, the size of the reduction current increases. The inset into Figure 2b is a plot of the charge under each of the reduction transients (Q_{Ru}) as a function of ruthenium deposition potential. The reduction charge is plotted as a ratio to 3 times the charge associated with a hydrogen monolayer on the platinum electrode ($3Q_H$). For deposition of a complete monolayer we would expect to see a ratio of 1, as reduction of the ruthenium complex requires 3 equiv of charge. For high deposition potentials ($E > 0.25$ V), we see that the deposition charge follows a linear relationship that would lead to close to one monolayer of deposited ruthenium being formed at 0 V. However, at 0.2−0.25 V, the Ru reduction charge starts increasing at a much faster rate, significantly exceeding the charge required to form a monolayer of Ru. At the lowest potential studied, the reduction charge would be enough to form over six monolayers of ruthenium.

There are two possible reasons for the latter observation. The first is that we are depositing multiple layers of ruthenium on the electrode; the second is that there is a homogeneous electrochemical reaction leading to the reduction of the ruthenium to a lower oxidation state, but not so far as to produce the zerovalent metal. The one-electron reduction of Ru^{III} to Ru^{II} shows a standard potential close to the potential at which the change in slope of the deposition charge/potential plot is seen[43]

$$Ru^{3+} + e^- \rightarrow Ru^{2+} \qquad E^{\ominus} = 0.2487 \text{ V} \qquad (7)$$

Relatively little work has been performed looking at the electrochemistry of the "$Ru(NO)(NO_3)_3$" species in acidic electrolyte, probably because in reality such solutions contain a range of components of the form $Ru(NO)(NO_3)_x(OH)_y$, where $x + y = 3$, the ratios of which depend on pH, temperature, etc. Bockris and Kim,[43] and before them Zvyagintsev and A. Kurbanov,[44] showed that the reduction of such solutions undergo three one-electron transfer steps, eventually leading to the production of metallic ruthenium. Thus it seems likely that the excessive reduction charge is merely the result of the partial reduction of the ruthenium complex to lower oxidation states that nonetheless remain soluble in solution and, thus do not contribute to the growth of more than a monolayer of ruthenium on the platinum electrode. This reaction does not occur until the potential is less than about 0.25 V. A parallel reaction, which starts at much higher potentials leads to the deposition of metallic ruthenium up to a coverage of one monolayer on the platinum electrode.

Further evidence for this assertion comes from cyclic voltammetry at a platinum rotating ring disk electrode (RRDE) in 0.5 mol dm^{-3} sulfuric acid in both the absence and presence of a 6.17×10^{-4} mol dm^{-3} $Ru(NO)(NO_3)_3$ solution, Figure 3. The disk currents are shown in Figure 3a, and the ring currents in Figure 3b. The ring potential was held at 0.456 V, i.e., a potential well below the formal potential of the $Ru^{III/IV}$ couple of 0.858 V,[11,42] but suitably high to result in the reoxidation of any species produced during the reduction of the "$Ru(NO)(NO_3)_3$" species. The disk potential was initially held at 1.456 V, a potential at which any deposited Ru would be dissolved off the platinum surface. The potential was then scanned down to 0.0 V and back up to 1.456 V at 0.050 V s^{-1}. In the absence of any $Ru(NO)(NO_3)_3$, the expected voltammetry of platinum is seen on the disk, and no currents are seen on the ring except at the lowest potential during which hydrogen produced on the disk is detected on the ring electrode.

In the presence of $Ru(NO)(NO_3)_3$ the voltammetry at both the disk and ring are significantly changed. At potentials below 0.32 V, a reduction is seen on the disk (i), although this does not lead to a limiting current plateau, suggesting that the reduction is under kinetic rather than diffusion control. Over the same potential range on the ring, an oxidation is seen, confirming that the reduction of the $Ru(NO)(NO_3)_3$ leads to a soluble species that can be reoxidized at the ring. There is a poorly defined current plateau on the ring, suggesting that the reoxidation process is more facile than the reduction reaction. Thus the deviation from the linear charge-potential line in the inset of Figure 2b is due to the homogeneous reduction of the "$Ru(NO)(NO_3)_3$" in the solution, and we can be confident that multiple layers of Ru are unlikely to be deposited on the Pt electrode.

The oxide reduction peak in the presence of $Ru(NO)(NO_3)_3$ is seen to shift by 100 mV in a cathodic direction from 0.75 V. This is probably due to the presence of some ruthenium on the electrode surface, deposited during the negative going scan.

Once the potential on the disk exceeds about 1.15 V, a poorly defined oxidation process is evident on the platinum disk (ii). It is also clear from the ring current over the potential range

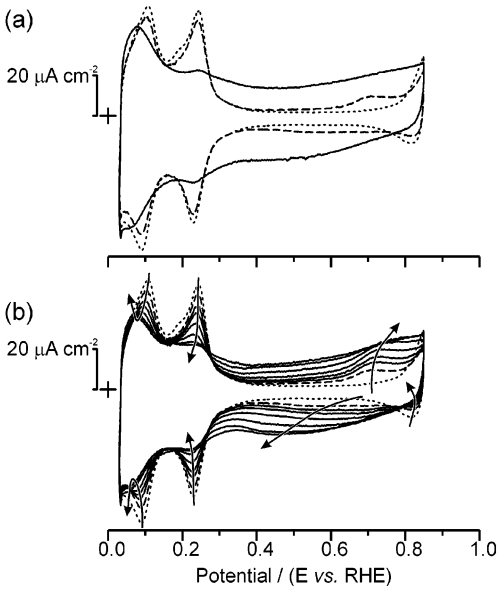

Figure 4. Cyclic voltammograms in 0.5 mol dm^{-3} sulfuric acid as a function of the amount of ruthenium deposited on a platinum electrode. $dV/dt = 0.1$ V s^{-1}. (a) Comparison between a bare platinum surface (···), a platinum surface with spontaneously deposited Ru (- - -), and a platinum surface the maximum amount of Ru deposited on it (E_{dep} = 0.006 V) (—). (b) Comparison between a bare platinum surface (···), a platinum surface with spontaneously deposited Ru (- - -), and platinum surfaces with progressively larger amounts of Ru deposited on them (E_{dep} = 0.506, 0.406, 0.356, 0.256, 0.181, and 0.131 V, respectively). Current densities are in terms of the geometric area of the underlying platinum electrode.

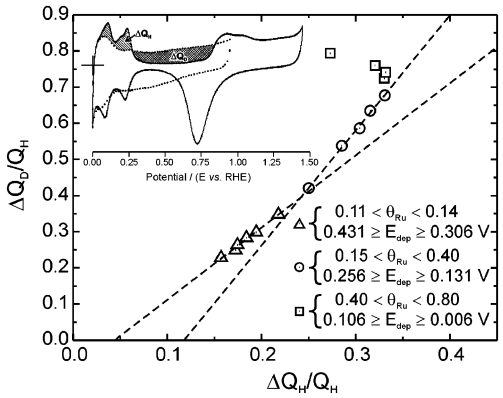

Figure 5. Plot of ruthenium oxide charge gained (ΔQ_D) versus hydrogen adsorption charge lost (ΔQ_H) for electrodes with different amounts of ruthenium deposited. In both cases the charges are normalized to the hydrogen adsorption charge of one monolayer on the clean platinum electrode (Q_H). Inset: cartoon showing the definition of the areas ΔQ_H and ΔQ_D. The voltammograms show the response of a pure platinum electrode (—), and a platinum electrode with some ruthenium deposited on it (···).

1.15−1.456 V that there is the reduction of a species produced on the disk. Thus oxidation of $Ru(NO)(NO_3)_3$ and any Ru on the electrode surface produces a soluble Ru^{IV} species that can be reduced at the ring back to Ru^{III} over this potential range.[42]

The impinging jet configuration has been shown to follow wall-jet like behavior, i.e., $i_{lim} \propto \nu^{3/4}$, where ν is the fluid velocity, although there is some debate as to whether it is a true wall-jet system.[36] Nonetheless, it is important to realize that this system will show a similar effect to that seen on the rotating disk system, i.e., that at low potentials we will see the homogeneous reduction of $Ru(NO)(NO_3)_3$, and that this process is responsible for the significant deviation in reduction charge seen in the inset diagram in Figure 2b. Such a process has also been seen in our laboratory during the reduction of $RuCl_3$ solutions, and indeed, Fredrich et al. suggest that the Faradaic deposition efficiency of Ru from $RuCl_3$ is less than 5%.[53]

3.2. Voltammetric Characterization of the Deposited Ru. Figure 4 shows voltammograms obtained in 0.5 mol dm^{-3} sulfuric acid after the deposition of Ru onto the platinum surface. Once Ru has been admitted to the platinum electrode surface, there is a marked difference in the voltammogram, with the features becoming more exaggerated as the amount of deposited Ru is increased. Figure 4a compares the voltammograms obtained on the bare platinum surface, the surface with spontaneously deposited Ru, and the surface with Ru deposited at the lowest potential, 0.006 V. The positive-most endpoint of the scan was chosen to be just at the point where oxide growth starts on platinum, and hence there is only a very small oxide reduction peak at 0.85 V on the pure platinum surface. Upon spontaneously depositing Ru on the platinum surface, it is seen that there is a small loss of charge in the hydrogen region, and there is the growth of a peak at 0.7 V. Furthermore, there is some growth of current in the double-layer region. In comparison, the surface with the largest amount of Ru deposited on it shows much larger currents in the double-layer region, and a significant depression of the strongly bound hydrogen peak at 0.25 V. There is also some decrease in the magnitude of the weakly bound hydrogen peak accompanied by a cathodic shift in potential.

Figure 4b details how the voltammetry changes as the amount of Ru on the surface varies between the limits described in Figure 4a. As the amount of Ru on the surface is increased, there is a suppression of the platinum oxide reduction peak followed by formation of a much broader reduction peak centered at about 0.5 V. The size of the strongly bound hydrogen peaks monotonically decreases with Ru coverage, but the weakly bound peaks initially decrease and then start to grow again at higher Ru coverage. The oxidation peak easily observed on the surface containing the spontaneously deposited Ru becomes broader and less well-defined as the amount of Ru on the surface increases and eventually blends in with the exaggerated double-layer feature.

For each ruthenium atom deposited onto a platinum site two separate distinguishable effects would be expected. The first is that a reduction in the hydrogen adsorption charge would be seen, as hydrogen does not adsorb to the same extent on Ru as it does on Pt. The second effect would be an increase in the charge seen in the double-layer region due to oxidation of that Ru atom. The change in size of the double layer is assumed to be as a result of the uniform oxidation of all Ru atoms to $Ru(OH)_2$ (eq 3), which is complete by the time the scan reaches its upper potential limit.[40] More explicitly, a linear relationship would be expected between the loss of H_{ads} charge, ΔQ_H, and the increase in charge within the double-layer region, ΔQ_D. Furthermore, in the case where no hydrogen would adsorb on the Ru atom in the hydrogen region, it would be expected that the charge in the double layer would increase at twice the rate at which the hydrogen charge decreases. The inset in Figure 5 shows how the hydrogen region decreases in size, and the double-layer region increases in size when the Pt electrode has some Ru deposited on it. In the main part of Figure 5 is a plot of ΔQ_D versus ΔQ_H, as a function of Ru deposition potential. Both ΔQ_D and ΔQ_H have been normalized to the hydrogen adsorption charge for the underlying platinum electrode. For comparison, the Ru surface coverage ranges are also displayed for these data points. These surface coverages were determined

using the Cu upd method and will be described in the following section. It can be seen that for the Ru layers deposited at high potentials, i.e., for those surfaces that have relatively little Ru on them (△), there is a good correlation between ΔQ_D and ΔQ_H, and the slope of the line is 2.0 ± 0.1. As the amount of Ru deposited increases (○), there is a break and the slope of the best fit line becomes 3.2 ± 0.1, indicating that either more charge is required to oxidize the Ru that is being deposited (i.e., it may be being oxidized to the +3 oxidation state) or, the more likely explanation, that the loss of hydrogen in the H-adsorption region is no longer exactly mirroring the addition of Ru to the surface. The latter is expected to occur because some hydrogen does adsorb onto the Ru surface and there is some extent of Ru oxidation occurring in the hydrogen adsorption region.[45] At still lower potentials (i.e., higher Ru coverage) (□), the ΔQ_H charge is seen to start decreasing again, almost certainly due to the effects mentioned above, and as a result no clear correlation between the oxide growth and loss of hydrogen adsorption charge can be determined.

If we accept the assumption made by Frelink et al., we may utilize the information presented in Figure 5, to determine θ_{Ru} by using eq 4. This process should provide a reasonable estimate of the Ru coverage until the point where it is obvious that there is no longer a good correspondence between the loss of hydrogen charge and the increase in Ru oxidation charge (i.e., for $E_{dep} > 0.106$ V). This approach will be utilized below and compared to the copper upd method.

3.3. Characterization of the Deposited Ru Using Copper upd. *3.3.1. The Copper upd Process.* In a previous paper we have shown that the stripping of upd Cu can be used as an accurate probe of the surface area of Pt and Ru both alone and in a PtRu alloy electrocatalyst.[29] Due to the size similarities of the lattice constants of copper, platinum and ruthenium, the copper is deposited in a 1:1 ratio on the substrate atoms irrespective of the Pt:Ru ratio.

The deposition and removal of a copper monolayer was carried out in the following manner and is represented schematically in the second part of the potential profile shown in Figure 1b. Once the Pt(Ru) electrode was prepared according to the procedure described above, the electrode potential was held at 0.3 V for 150 s. This potential was chosen because it is just high enough to prevent bulk deposition of Cu, but is low enough to provide a surface on which the majority of Ru is reduced. A 50 s dose of 1.08×10^{-3} mol dm^{-3} $CuSO_4$ in 0.5 mol dm^{-3} sulfuric acid solution was injected into the electrolyte flow. The resulting chronoamperograms for a range of different Pt(Ru) electrodes are shown in Figure 6a. In this diagram during period i, only the 0.5 mol dm^{-3} sulfuric acid background electrolyte flows over the surface. During period ii, the Cu-containing solution flows over the surface, and during period iii the solution is again only background electrolyte. During period ii a transient due to the deposition of Cu on the electrode is seen. This transient decays to a small background level while Cu containing solution is still flowing over the surface, indicating the adsorbed Cu layer completely forms within about 20 s under the conditions used.

During period (iii) a small peak is seen in the chronoamperograms, indicating that some of the copper that was deposited during step ii is removed when only sulfuric acid is present. The charges involved are around 2% on pure platinum and increase with Ru content, up to about 9% of the charge in the main deposition peak. The process would appear to be due to the equilibrium that is set up between the upd Cu and cupric ions in the adjacent solution. Currently, it is not possible to determine whether this extra charge is due to a small component of Cu multilayer formation or if it is due to the lack of stability of a complete monolayer of Cu in equilibrium with 0.5 mol dm^{-3} sulfuric acid solution at 0.3 V. The implication of this observation is that our measurements of surface area using Cu upd may represent an underestimate by several percent. We find that using the deposition chronoamperograms is relatively unsatisfactory for performing further calculations, as they are significantly affected by any background currents due to the relatively long times over which the transients are collected, and instead, we rely on linear sweep stripping voltammograms to characterize the surface and determine the surface area of each of the precious metal components on our electrodes.

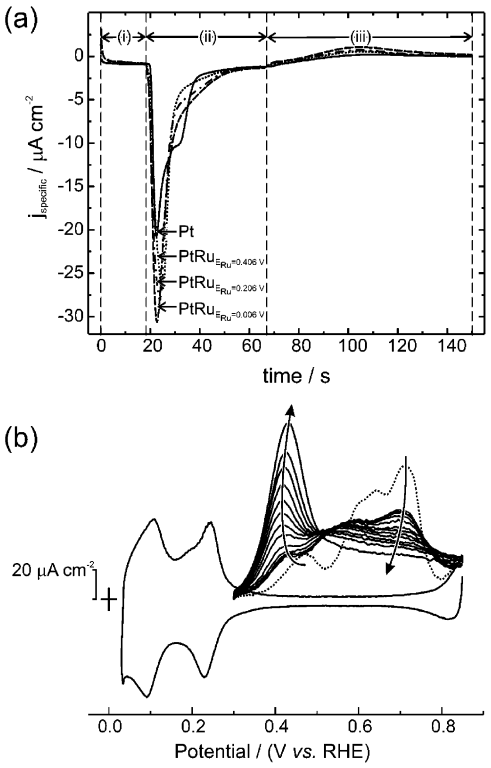

Figure 6. Copper upd adsorption transients (a) and copper stripping voltammograms (b) for a Pt electrode with different amounts of Ru deposited upon it. Adsorption transients were performed in 0.5 mol dm^{-3} sulfuric acid background electrolyte in the presence of 1.08×10^{-3} mol dm^{-3} $CuSO_4$. The transients show copper adsorption on the Pt electrode (—) and on the Pt electrode with Ru deposited at 0.406 V (•••), 0.206 V, and 0.006 V (– – –). The voltammograms show copper stripping in the absence of any Cu^{2+} in solution. dE/dt = 0.10 V s^{-1}.

Figure 6b shows the stripping voltammograms performed immediately after the adsorption transients of Figure 6a. The potential was swept from the hold potential of 0.3 V to 0.85 V at 0.1 V s^{-1} under flowing 0.5 mol dm^{-3} sulfuric acid solution. During this linear scan voltammetry the copper deposit was oxidatively removed from the electrode surface. Potential scans after this first linear scan detected no copper on the surface. For each Ru deposition potential used, voltammograms were recorded for the cleaned platinum surface, for the ruthenium-covered surface, and for the removal of the copper deposit. It can immediately be seen that the voltammetric process of removal of the copper deposit from all the electrodes studied occurs completely within the double-layer region and that there is a progressive yet marked difference in the profile of the peaks as the composition of the electrodes becomes more Ru rich.

The removal of the copper deposit from the bare platinum electrode shows a similar voltammetric picture to that discussed

previously for the large polycrystalline platinum electrode.[29] Four peaks can be distinguished, with their ratios differing slightly from those in ref 29 due to the nanoparticulate nature of the Pt used in the previous work, resulting in slightly different ratios of the Cu adsorption sites. Once Ru is introduced onto the platinum surface, there is a considerable change in the copper stripping voltammetry. The peaks become much broader and commence at lower potentials. As the amount of Ru deposited on the electrode surface is increased, there is a gradual increase in the size of the first peak and a decrease in the size of the broader peaks occurring at higher potentials.

In our previous paper we showed that the first peak, at around 0.42 V was due to removal of the copper deposit from Ru sites alone and that the broader feature at higher potential was removal from the Pt sites. This aspect has been discussed extensively and requires no further mention here.[29]

3.3.2. Surface Area Determination Using Cu upd and CO Stripping. Calculation of the charge due to stripping of an adsorbed Cu upd layer is made more difficult due to anion adsorption and double-layer effects. During a stripping experiment, the total charge measured, Q_{exp}, will be the sum of these and other charges:

$$Q_{exp} = Q_{upd} + Q_{DL} + Q_{anion} + Q_{oxide} \quad (8)$$

where Q_{upd} is the charge due to the copper upd layer and is assumed to be 420 μC cm^{-2} on polycrystalline platinum[46] (cf. 480 mC cm^{-2} for Cu on Pt(111)[46]), Q_{DL} is the charge due to charging of the double-layer capacitance of the electrode, Q_{anion} is the charge due to adsorption/desorption of specifically adsorbed anions, and Q_{oxide} is the charge due to the growth of any oxide or adsorption of any oxygenated species.

A particularly elegant methodology to deconvolute Cu deposition from anion adsorption effects and double-layer charging using rotating ring−disk voltammetry has been presented by Markovic et al. in their study of copper deposition on Pt(111).[47] For their approach it is necessary to use low concentrations of copper (otherwise the collection efficiency may change during the experiment due to excessive Cu deposition in the ring), and as a result the use of low Cu concentrations will limit the maximum coverage attainable. Furthermore, their approach is not amenable to in situ deposition and study of the Pt(Ru) surfaces as produced in this study.

In our experiments, we have corrected our experimentally measured charges for the last three terms in eq 8 by subtracting from the Cu upd stripping charge the charge obtained for a linear potential scan for the same electrode over the same potential range (0.3 → 0.85 V) in the absence of any Cu^{2+} in solution. In order for this approach to be valid, the end potential must be beyond the point at which any Cu remains on the surface, and we must assume that both the double-layer capacitance and anion adsorption coverage are similar on the electrode surfaces. Although the former is a good approximation,[32] some small error may be introduced by the latter assumption, although the situation is complicated due a paucity of experimental data at high sulfate concentrations.[46,48] We will consider anion adsorption effects in a future paper.[49] In the case of CO adsorption, both Q_{DL} and Q_{anion} are significantly different at the CO adsorption potential, and so it is important to correct for these effects by measuring the anion displacement charge during CO adsorption, as is easily accomplished using the impinging jet apparatus.[38]

Figure 7 shows the variation of roughness factor (specific/geometric surface area) for our electrode as a function of the Ru deposition potential. Also displayed in this diagram are the

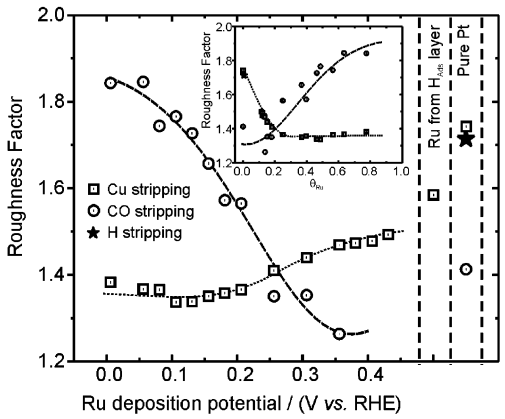

Figure 7. Variation of electrode roughness factor (specific area/geometric area) as a function of Ru deposition potential determined using Cu upd (□), CO stripping (○), and hydrogen stripping (★). Inset: variation of roughness factor with Ru coverage as determined by Cu upd.

surface areas determined for our Pt electrode with no Ru deposited upon it and for a Pt(Ru) electrode produced via the ionization of a preadsorbed hydrogen layer on the Pt. For comparison we also include the surface area determined through stripping of an adsorbed CO layer. The CO was adsorbed on the Pt(Ru) electrode after it had been characterized, by holding the potential at 0.3 V for 200 s and changing the flowing electrolyte for one saturated in CO for 50 s within this period. Under these conditions a saturated coverage of CO is formed within 5 s. The CO was then stripped off the surface by applying a potential ramp to 1.20 V at 0.050 V s^{-1}. No CO was detected on the surface during a second voltammetric scan performed immediately after the first. A number of features are evident in this diagram. The first is that on pure Pt the Cu upd method gives a surface area very close to that observed using the hydrogen adsorption technique. Indeed, others have reported high coverages ($\geq$0.8) of upd Cu on polycrystalline platinum in other electrolytes.[46] In comparison we see a CO coverage of only about 80% of the hydrogen area, a reasonable value when compared to saturated coverages of 0.64 on Pt(111) and 0.82 for both Pt(100) and Pt(110),[50,51] determined at the same adsorption potential. Adsorption of even a small amount of Ru results in the loss of some surface area, as determined by Cu stripping, but the resultant surface shows only a small further change in surface area as the amount of deposited Ru is increased. The roughness factor calculated from CO stripping also shows a drop when small amounts of Ru are deposited on the surface and furthermore still shows about 80% of the surface area as seen with the Cu upd technique. However, as the amount of Ru on the surface increases, the effective surface area measured by CO stripping increases, overtaking that measured by the Cu upd technique and resulting in a 35% increase in measured surface area when compared to the Cu upd technique.

This result suggests that the coverage of CO on Pt(Ru) catalysts is composition dependent and that using a conversion factor of 420 μC cm^{-2} to convert stripping charge into real surface area may result in significant errors, especially for systems with high Ru surface coverage.

3.3.3. Ru Coverage Determined through Cu upd. In a previous paper we have shown how it is possible to determine the Ru metal surface content of a Pt(Ru) catalyst using the Cu upd method.[29] In this paper we use a simplified version of our previous approach to determine surface composition according to the removal of an upd Cu monolayer. The total charge under

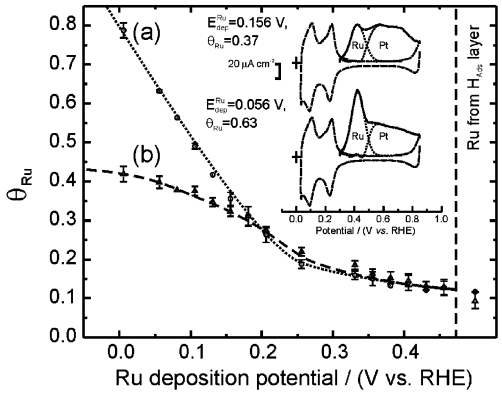

Figure 8. Variation of Ru coverage with Ru deposition potential as determined using the Cu upd technique (a) and the oxide formation process (b). See text for further details. Inset: Detail of the deconvolution of the Cu upd stripping peaks into an Ru component and a Pt component for Ru deposited at two different potentials, 0.156 V (θ_{Ru} = 0.37) and 0.056 V (θ_{Ru} = 0.63).

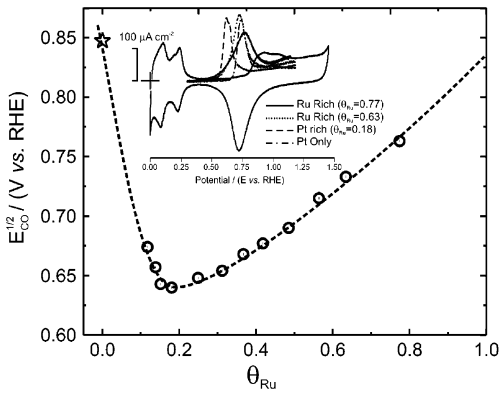

Figure 9. Variation of potential at which half of a saturated CO layer has been oxidized (E_{CO}) versus Ru coverage for the oxidation of a CO adlayer adsorbed at 0.25 V in 0.5 mol dm^{-3} sulfuric acid. Inset: stripping curves for surfaces with different Ru coverages. dE/dt = 0.05 V s^{-1}.

the first anodic feature was determined by deconvoluting that peak assuming it had a Gaussian line shape. This approach gives a very good fit to the initial peak over a wide range of Ru coverages, with two examples of the deconvolution displayed inset in Figure 8. The Ru coverage was then determined from the ratio of charge in the first peak compared to the total Cu upd stripping charge.

$$\theta_{Ru} = \frac{Q_{\mathrm{Ru}}^{\mathrm{Cu_{upd}}}}{Q_{\mathrm{Tot}}^{\mathrm{Cu_{upd}}}} \tag{9}$$

Displayed in Figure 8 is a plot of Ru coverage with Ru deposition potential calculated from both the oxide coverage and from the deconvolution of the Cu upd peaks. Error bars are calculated from measurements made over three independent experiments. Over the potential range for which there is a good correspondence between the loss of hydrogen charge with growth of Ru oxide charge (see Figure 5), i.e., $E > 0.13$ V, there is good agreement between the Ru surface coverage measured using each method. When more Ru is deposited, i.e., for $E \leq 0.13$ V, there is significant divergence in the Ru coverage measured by the two different methods. As previously described, the method for determining Ru coverage from the oxide charge appears to show a significant divergence from what we might expect, as has been shown in Figure 5. Indeed, Frelink et al.[2] restricted the use of this technique to surfaces with Ru coverages less than about 0.4, exactly where we see such a divergence. Furthermore, the Ru coverage measured using the oxide charge appears unusually low, especially when compared to the expected coverage as determined from the extrapolated Ru deposition charge in Figure 2. We attribute the discrepancy as being due to significant hydrogen adsorption occurring on the Ru when the Ru coverage is greater than 0.4.

In comparison, the Ru surface coverage measured using the Cu upd technique agrees qualitatively with the extrapolated Ru deposition charge (dashed line in the inset in Figure 2b). We thus conclude that the Cu upd technique provides a good measure of the Ru surface content over a wider range of surface compositions than the technique utilizing the oxide charge. Utilizing the Ru coverage as calculated by the Cu upd technique, we may replot the data in Figure 7 in terms of the Ru surface coverage, this is shown inset of Figure 7.

3.4. Activity toward CO and Methanol Oxidation as a Function of θ_{Ru}. In the previous section we have shown that it is possible to utilize the Cu upd technique to determine the Ru coverage of our Pt(Ru) electrodes, and so this allows us to determine the optimum composition of electrodes for various reactions. The Pt(Ru) electrode was prepared and characterized as described previously, and then the potential was held at 0.1 V. The electrolyte solution was changed from the 0.5 mol dm^{-3} sulfuric acid background electrolyte to one containing the background electrolyte and the species of interest.

3.4.1. Oxidation of a Saturated CO Adlayer as a Function of Ru Content. A saturated layer of CO on the surface of the electrode was produced as previously described in 3.3.1. The potential was then scanned at 0.05 V s^{-1} to 1.2 V. Displayed in Figure 9 is a plot of the potential at which half the CO oxidation charge had been consumed, $E_{CO}^{1/2}$ as a function of Ru coverage. This potential was found to give a more consistent, although qualitatively similar, result to the potential of the peak current, as for the latter a double peak was often observed for some electrode compositions. The $E_{CO}^{1/2}$ value decreases very quickly as Ru is added to the surface and shows a minimum for a Ru coverage of 0.18. As the Ru content is increased above this value, the activity of the surface toward oxidation of the adsorbed CO layer slowly decreases, tending toward a value that is slightly below the value for pure platinum. Thus it is seen that the bimetallic composition of the surface has a synergetic effect for the oxidation of CO compared to each of the individual elements. Displayed in the inset in Figure 9 are a number of the stripping voltammograms at different Ru coverages. Pt rich surfaces display much sharper stripping peaks than Ru rich surfaces.

3.4.2. Oxidation of Methanol as a Function of Ru Content. After preparation of the electrode as previously described, and polarization of the electrode at 0.1 V, the electrolyte solution was changed to one containing 0.5 mol dm^{-3} sulfuric acid + 0.5 mol dm^{-3} methanol. Immediately after the methanol had reached the electrode surface, the potential was stepped to 0.5 V and the current measured over a 1500 s period. The experiment was repeated for the full range of Ru−Pt compositions. Figure 10 shows a set of representative current transients as a function of Ru surface content. Currents are reported as specific activities, with the surface area of each electrode determined from the Cu upd stripping charges on that electrode. In all cases the transients are characterized by an initial current peak, typically occurring 30−50 s after polarization, and then a drop in current which at times greater than 500 s may be approximated by a linear decay, as shown by the dashed lines.

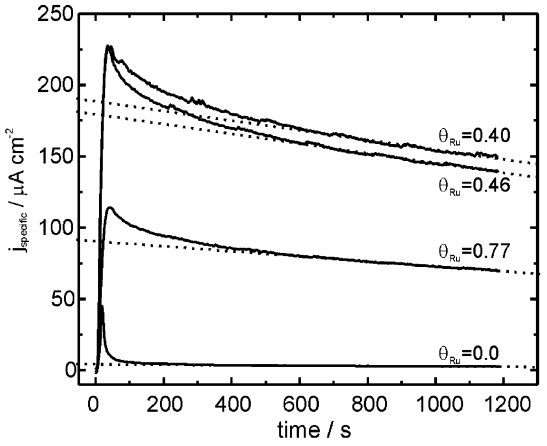

Figure 10. Chronoamperometric transients for the oxidation of 0.5 mol dm^{-3} methanol in 0.5 mol dm^{-3} sulfuric acid at 25 °C on electrodes with ruthenium coverages of 0, 0.4, 0.46, and 0.77 monolayer. Specific surface areas for each electrode were determined by Cu upd.

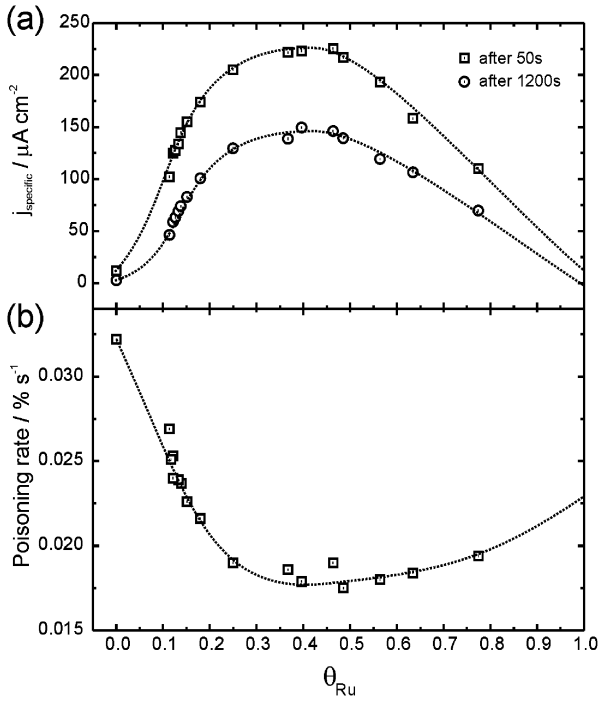

Figure 11. Specific current density at 50 s and 1200 s (a) and poisoning rate (b) for the oxidation of 0.5 mol dm^{-3} methanol in 0.5 mol dm^{-3} sulfuric acid at 25 °C on PtRu electrodes as a function of Ru coverage. Specific surface areas for each electrode were determined by Cu upd.

For pure platinum, the current peak is shifted to shorter times and is followed by a significant loss in activity before the linear section is reached. In comparison, as the Ru coverage increases, the extent of the drop after the current maximum decreases. Figure 11a displays the variation of specific activity with electrode composition at two different polarization times, 50 and 1200 s. Both curves follow the same trend, implying that the poisoning mechanism probably remains quite similar across all electrodes studied. As was seen for the case of CO oxidation, the addition of Ru to a pure Pt surface has a much greater effect than the addition of Pt to a Ru surface, as can be judged by the slope of the specific activity−composition curves when extrapolated to either edge of the graph. Maximum activity is seen at Ru compositions in the range 0.25−0.5, in agreement with similar studies on Ru electrochemically deposited on Pt.[16,17]

The linear decay of the current at times greater than 500 s may be characterized by the long-term poisoning rate, δ:[52]

$$\delta = \frac{100}{i_0} \times \left(\frac{\mathrm{d}i}{\mathrm{d}t}\right)_{t>500\mathrm{s}} (\% \ \mathrm{s}^{-1}) \qquad (10)$$

where $(\mathrm{d}i/\mathrm{d}t)_{t>500}$ is the slope of the linear portion of the current decay, and i_0 is the current at the start of polarization back extrapolated from the linear current decay. Figure 11b plots the variation of this parameter as a function of Ru surface coverage. Again a pronounced effect is seen upon adding Ru to the Pt surface, with a rapid decrease in poisoning rate seen as the Ru coverage increases. In comparison, at Ru coverages greater than 0.4, the poisoning rate hardly changes at all, suggesting that the addition of Ru to the surface is not significantly affecting the buildup of poisons on the surface.

Friedrich et al.[53] and Herrero et al.[54] have used STM to probe the morphology of Ru electrodeposited from $RuCl_3$ solutions onto single-crystal platinum electrodes. In both cases they note the formation of islands, 1−3 nm in diameter, typically of monatomic height, but with a small percentage (<10%) of two atoms height. In comparison, it is usually assumed that alloy electrocatalysts show a purely statistical distribution of Pt and Ru atoms on their surface.[12] Thus even though the surface composition is the same, the precise configuration of the surface atoms may be quite different in the two systems, begging the question as to whether the results determined on the former are applicable to the latter. Ultimately, this becomes a question of how quickly adsorbed intermediates may diffuse across the surface to find a suitable reaction site; in the case where we have islands of material, this diffusion time may become considerable if the surface diffusion coefficient is small. For the case of CO, Friedrich et al.[53] estimate a value of 10^{-13} to 10^{-12} cm^2 s^{-1}, suggesting that with such small islands it is possible, to a first approximation, to apply the results determined from such systems to the "statistically distributed" PtRu surfaces typically used as real electrocatalysts.

4. Conclusions

In this paper we have shown how it is possible to deposit submonolayer amounts of Ru onto a polycrystalline Pt bead electrode from a $RuNO(NO_3)_3$ solution using an impinging jet apparatus. The impinging jet flow cell method affords easy manipulation of the electrolyte while potential control is maintained over the electrode at all times. Deposition of 0.12 ± 0.2 monolayer of Ru is seen on a reduced platinum surface due to reaction of the adsorbed hydrogen on the platinum. The deposition process is complicated by the simultaneous solution-based reduction of the Ru precursor to a soluble product. This means that we cannot use the Ru deposition charge to determine the amount of Ru present on the electrode surface.

For low coverages of surface ruthenium, the surface composition determined through the removal of an underpotential deposited monolayer of copper agrees well with existing electrochemical techniques utilizing the growth of oxide on Ru over the double-layer potential range. At high coverage the method is a significant improvement, as oxide growth significantly impinges on the hydrogen adsorption region, resulting in an underestimate of the amount of Ru deposited. The inability of the oxide method to distinguish surface coverages greater than 30% is evidenced not only by the Cu upd voltammetry but also by a significant change in the ratio of charge lost in the hydrogen region to charge gained in the double-layer region. Furthermore, the significant changes in electrocatalytic activity

seen for electrodes in which the Ru was deposited at lower potentials is not reconcilable with the Ru surface coverage of 0.3−0.4, as suggested by the integrated oxide charge.

Although we have not unequivocally shown that the Ru on the surface is in the form of islands of monatomic height, such an assessment would be reasonable in light of previous work carried out utilizing Ru deposited from $RuCl_3$ solutions onto single-crystal Pt. Nonetheless, we can be certain that we do not have the formation of bulk three-dimensional deposits on the basis of the constancy of total surface area with Ru coverage as measured by the Cu upd technique.

The oxidation process for a saturated layer of CO is seen to change significantly as the coverage of Ru changes. Not only does the activity of the surface change, showing a maximum for a surface with a Ru coverage of 0.2, but also the total amount of CO adsorbed is found to increase as the Ru coverage increases. This would seem to suggest that the coverage of CO on the Pt(Ru) surface is composition dependent and cannot be assumed to be the same as for a pure Pt surface. This may be due to a change in the bonding mechanism of CO on going from a pure Pt surface to one predominantly covered with Ru.

For the oxidation of methanol at 0.5 V and 25 °C, it is found that there is a broad maximum in catalytic activity for Ru coverages in the range 0.25−0.5. Over this variation in composition the current changes by less than 10%. The long-term poisoning rate (i.e., rate of poisoning at times longer than 500 s) shows a minimum for surfaces that are richer in Ru, extending from 0.4 all the way to ∼0.6. We are currently examining results for the short-term poisoning rate as a function of composition and looking at more accurate measurements of the anion adsorption charge on these systems.

Acknowledgment. The expertise provided by Mr. Steve Atkins (Department of Chemistry, Imperial College) in constructing electronic equipment is gratefully acknowledged. In addition, C.L.G. thanks the EPSRC of the U.K. for a quota studentship.

References and Notes

(1) Watanabe, M.; Motoo, S. *J. Electroanal. Chem.* **1975**, *60*, 267−273.
(2) Frelink, T.; Visscher, W.; vanVeen, J. A. R. *Langmuir* **1996**, *12*, 3702.
(3) Arico, A. S.; Srinivasan, S.; Antonucci, V. *Fuel Cells* **2001**, *1*, 133.
(4) Curran, C. *Chem. Ind.−London* **2001**, *23*, 767.
(5) Raadschelders, J. W.; Jansen, T. *J. Power Sources* **2001**, *96*, 160.
(6) Ravikumar, M. K.; Kucernak, A. Unpublished results.
(7) Reddington, E.; Sapienza, A.; Gurau, B.; Viswanathan, R.; Sarangapani, S.; Smotkin, E. S.; Mallouk, T. E. *Science* **1998**, *280*, 1735.
(8) Ross, P. N. *Electrochim. Acta* **1991**, *36*, 2053.
(9) Tremiliosi, G.; Kim, H.; Chrzanowski, W. *J. Electroanal. Chem.* **1999**, *467*, 143.
(10) Xia, X. H.; Iwasita, T.; Ge, F.; Vielstich, W. *Electrochim. Acta* **1996**, *41*, 711.
(11) McNicol, B. D.; Short, R. T. *J. Electroanal. Chem.* **1977**, *81*, 249.
(12) Gasteiger, H. A.; Markovic, N.; Ross, P. N.; Cairns, E. J. *J. Phys. Chem.* **1994**, *98*, 617.
(13) Watanabe, M.; Uchida, M.; Motoo, S. *J. Electroanal. Chem.* **1987**, *229*, 395.
(14) Frelink, T.; Visscher, W.; vanVeen, J. A. R. *Surf. Sci.* **1995**, *335*, 353.
(15) Gasteiger, H. A.; Markovic, N.; Ross, P. N.; Cairns, E. J. *J. Phys. Chem.* **1993**, *97*, 12020.
(16) Iwasita, T.; Hoster, H.; John-Anacker, A.; Lin, W. F.; Vielstich, W. *Langmuir* **2000**, *16*, 522.
(17) Hoster, H.; Iwasita, T.; Baumgartner, H.; Vielstich, W. *Phys. Chem. Chem. Phys.* **2001**, *3*, 337.
(18) Chrzanowski, W.; Wieckowski, A. *Langmuir* **1998**, *14*, 1967.
(19) Gasteiger, H. A.; Markovic, N.; Ross, P. N.; Cairns, E. J. *J. Electrochem. Soc.* **1994**, *141*, 1795.
(20) Maniguet, S.; Mathew, R. J.; Russell, A. E. *J. Phys. Chem. B* **2000**, *104*, 1998.
(21) Russell, A. E.; Maniguet, S.; Mathew, R. J.; Yao, J.; Roberts, M. A.; Thompsett, D. *J. Power Sources* **2001**, *96*, 226.
(22) Chrzanowski, W.; Wieckowski, A. *Langmuir* **1997**, *13*, 5974.
(23) Brankovic, S. R.; McBreen, J.; Adzic, R. R. *J. Electroanal. Chem.* **2001**, *503*, 99.
(24) Brankovic, S. R.; Wang, J. X.; Adzic, R. R. *Electrochem. Solid State Lett.* **2001**, *4*, 217−220.
(25) Vigier, F.; Gloaguen, F.; Leger, J. M.; Lamy, C. *Electrochim. Acta* **2001**, *46*, 4331.
(26) Dinh, H. N.; Ren, X.; Garzon, F. H.; Zelenay, P.; Gottesfeld, S. *J. Electroanal. Chem.* **2000**, *491*, 222.
(27) Hadži-Jordanov, S.; Angerstein-Kowlowska, H.; Vukovič, M.; Conway, B. E. *J. Electrochem. Soc.* **1978**, *125*, 1471.
(28) Lezna, R. O.; De Tacconi, N. R.; Arvía, A. J. *J. Electroanal. Chem.* **1983**, *151*, 193.
(29) Green, C. L.; Kucernak, A. *J. Phys. Chem. B* **2002**, *106*, 1036.
(30) Tindall, G. W.; Bruckenstein, S. *Anal. Chem.* **1968**, *40*, 1051.
(31) Bowles, B. J. *Electrochim. Acta* **1970**, *15*, 589.
(32) Schultze, W. J. *Ber. Bunsen-Ges. Phys. Chem.* **1970**, *74*, 705.
(33) Scortichini, C. L.; Reiley, C. N. *J. Electroanal. Chem.* **1982**, *139*, 233.
(34) Quiroz, M. A.; Meas, Y.; Lamy-Pitara, E.; Barbier, J. *J. Electroanal. Chem.* **1983**, *157*, 165.
(35) Chrzanowski, W.; Kim, H.; Tremiliosi-Filho, G.; Wieckowski, A.; Grzybowska, B.; Kulesza, P. *J. New Mater. Electrochem. Syst.* **1998**, *1*, 31.
(36) Bergelin, M.; Wasberg, M. *J. Electroanal. Chem.* **1998**, *449*, 181.
(37) Bergelin, M. Personal communication.
(38) Bergelin, M.; Feliu, J. M.; Wasberg, M. *Electrochim. Acta* **1998**, *44*, 1069.
(39) Bergelin, M.; Herrero, E.; Feliu, J. M.; Wasberg, M. *J. Electroanal. Chem.* **1999**, *467*, 74.
(40) Koponen, U.; Peltonen, T.; Bergelin, M.; Mennola, T.; Valkiainen, M.; Kaskimies, J.; Wasberg, M. *J. Power Sources* **2000**, *86*, 261.
(41) Szabó, S.; Bakos, I. *J. Electroanal. Chem.* **1987**, *230*, 233.
(42) De Zourbov, N.; Pourbaix, M. *Atlas of electrochemical equilibria in aqueous solution*; National Association of Corrosion Engineers: Houston, TX, 1966; Section 13.1.
(43) Bockris, J. O.; Kim, J. *J. Electrochem. Soc.* **1996**, *143*, 3801.
(44) Zvyagintsev, O. E.; Kurbanov, A. *Zh. Neorg. Khim.* **1958**, *3*, 2305.
(45) Hadži-Jordanov, S.; Angerstein-Kowlowska, H.; Vukovič, M.; Conway, B. E. *J. Phys. Chem.* **1977**, *81*, 2271.
(46) Varga, K.; Zelenay, P.; Wieckowski, A. *J. Electroanal. Chem.* **1992**, *330*, 453.
(47) Markovic, N. M.; Gasteiger, H. A.; Ross, P. N. *Langmuir* **1995**, *11*, 4098.
(48) Horanyi, G. *Electroanal. Chem. Interfacial Electrochem.* **1974**, *55*, 45.
(49) Green, C.; Kucernak, A. Manuscript in preparation.
(50) Lebedeva, N. P.; Koper, M. T. M.; Herrero, E.; Feliu, J. M.; van Santen, R. A. *J. Electroanal. Chem.* **2000**, *487*, 37.
(51) Gómez, R.; Feliu, J. M.; Aldaz, A.; Weaver, M. J. *Surf. Sci.* **1998**, *410*, 48.
(52) Jiang, J.; Kucernak, A. *J. Electroanal. Chem.* **2002**, *520*, 64.
(53) Friedrich, K. A.; Geyzers, K.-P.; Marmann, A.; Stimming, U.; Vogel, R. *Z. Phys. Chem.* **1999**, *208*, 137.
(54) Herrero, E.; Feliu, J. M.; Wieckowski, A. *Langmuir* **1999**, *15*, 4944.